Journal of Oceanography, Vol. 62, pp. 155 to 170, 2006

Steric Sea Level Changes Estimated from Historical Ocean Subsurface Temperature and Salinity Analyses

MASAYOSHI ISHII[1]*, MASAHIDE KIMOTO[2], KENJI SAKAMOTO[3] and SIN-ITI IWASAKI[4]

[1]*Frontier Research Center for Global Change, Japan Agency for Marine-Earth Science and Technology, Yokohama 236-0001, Japan*
[2]*Center for Climate System Research, University of Tokyo, Kashiwa 277-8586, Japan*
[3]*Climate Prediction Division, Japan Meteorological Agency, Tokyo 100-8122, Japan*
[4]*National Research Institute for Earth Science and Disaster Prevention, Tsukuba 305-0006, Japan*

(Received 29 August 2005; in revised form 12 November 2005; accepted 28 November 2005)

An historical objective analysis of subsurface temperature and salinity was carried out on a monthly basis from 1945 to 2003 using the latest observational databases and a sea surface temperature analysis. In addition, steric sea level changes were mainly examined using outputs of the objective analyses. The objective analysis is a revised version of Ishii et al. and is available at 16 levels in the upper 700 m depth. Artificial errors in the previous analysis during the 1990s have been worked out in the present analysis. The steric sea level computed from the temperature analysis has been verified with tide gauge observations and TOPEX/Poseidon sea surface height data. A correction for crustal movement is applied for tide gauge data along the Japanese coast. The new analysis is suitable for the discussion of global warming. Validation against the tide gauge reveals that the amplitude of thermosteric sea level becomes larger and the agreement improves in comparison with the previous analysis. A substantial part of local sea level rise along the Japanese coast appears to be explained by the thermosteric effect. The thermal expansion averaged in all longitudes from 60°S to 60°N explains at most half of recent sea level rise detected by satellite observation during the last decade. Considerable uncertainties remain in steric sea level, particularly over the southern oceans. Temperature changes within MLD make no effective contribution to steric sea level changes along the Antarctic Circumpolar Current. According to statistics using only reliable profiles of the temperature and salinity analyses, salinity variations are intrinsically important to steric sea level changes in high latitudes and in the Atlantic Ocean. Although data sparseness is severe even in the latest decade, linear trends of global mean thermosteric and halosteric sea level for 1955 to 2003 are estimated to be 0.31 ± 0.07 mm/yr and 0.04 ± 0.01 mm/yr, respectively. These estimates are comparable to those of the former studies.

Keywords:
· Temperature analysis,
· salinity analysis,
· steric sea level,
· TOPEX/Poseidon,
· tide gauge,
· crustal movement.

1. Introduction

The roles of oceans as a huge reservoir of heat and water are important in the global climate system. Global warming is now proceeding, and therefore it becomes increasingly important to understand what happened in the global oceans during the last century. Recent studies suggest warming of the world oceans; Levitus *et al.* (2005b; LAB05, hereafter) reported that the temperature of the global oceans in the upper 3000 m depths has increased by 0.037°C during the period between 1955 and 1998. After the publication of the Third Assessment Report by the Intergovernmental Panel on Climate Change in 2001 (IPCC TAR), global mean sea level rise (SLR) has been studied intensively in collaboration with various communities relevant to geophysics and astronomy (Cazenave and Nerem, 2004). Recently, Antonov *et al.* (2005) estimated a trend of global mean thermosteric sea level, due to thermal expansion, of 0.33 mm/yr using the temperature analysis of LAB05. This estimate is about 5 times smaller than 1.84 mm/yr computed from tide gauge

* Corresponding author. E-mail: ism@jamstec.go.jp
On leave from the Meteorological Research Institute of the Japan Meteorological Agency.

data (Douglas and Peltier, 2002), although the tide gauge observations are poorly distributed in space and the data suffer from crustal movement at the stations (Cazenave and Nerem, 2004). In contrast, the estimate of global sea level trend from tide gauge data is not significantly different when an isostatic adjustment is taken into account (Peltier, 2001). For the period from 1993 to 2003, recent studies show that thermosteric sea level rise is around 1.2–1.5 mm/yr (Willis *et al*., 2004; Antonov *et al*., 2005), while an analysis of the TOPEX/Poseidon sea surface height (Chambers *et al*., 2003) shows a doubled trend of 2.8 mm/yr for the same period (Cazenave and Nerem, 2004). To explain the smaller trends of thermosteric sea level than those of the direct sea level measurement, Antonov *et al*. (2002) suggested that input of fresh water to the oceans explains the remainder of sea level rise on the basis of evidence of salinity freshening in their salinity analysis. However, large uncertainty remained in the estimation of SLR (Church *et al*., 2001) since the water circulation between climate subsystems of atmosphere, ocean, and land surface is quantitatively unknown. The characteristics of thermosteric sea level variations on decadal time scales over the global oceans are examined by Lombard *et al*. (2005) comparing two historical temperature analyses by Levitus *et al*. (2000) and Ishii *et al*. (2003; IKK03, hereafter). In particular, the thermosteric sea levels vary in phase with dominant modes of climate variability such as El Niño and the Southern Oscillation, Pacific Decadal Oscillation (PDO), and North Atlantic Oscillation. Stephens *et al*. (2001) also reported that Pacific Ocean heat content changes in phase with PDO.

The present study follows IKK03 in which a historical objective analysis of oceanic temperature was carried out on a monthly basis for the period from 1950 to 1998. A major purpose is to make an objective analysis of temperature and salinity for use in climate studies. The previous analysis scheme is improved for better representation of climate variations, and the new objective analysis is applied to examine historical sea level changes. Errors in steric sea level are also estimated. One concern of this investigation is how the geographic distribution of climate anomalies is reproduced whereas only the spatio-temporal averages are discussed in the pioneering researches mentioned above. In addition, local changes in sea level are of great concern here as this is one of serious problems under global warming for human beings. Oceanographical observations suffer from noise and lack of representativeness due to the existence of meso-scale eddies. These affect the ocean analyses and interpreting such an analysis may not be easy. The analysis scheme used in this study is based on a recent methodology of objective analysis (Derber and Rosati, 1989; Ghil and Malanotte-Rizzoli, 1991), and is superior in reducing observational noise in a resultant analysis as described in IKK03 and Section 2. Similar objective analysis schemes based on optimal interpolation have been applied to SST analyses (Reynolds and Smith, 1994; Ishii *et al*., 2005), and are successful in reducing the observational noise in SST data.

The objective analysis of monthly ocean subsurface temperature by IKK03 has several deficiencies, mainly due to the mixture of observational databases of subsurface temperature and sea surface temperature (SST). Although the analysis shows good agreement with Levitus *et al*., 2000) according to the above-mentioned comparison study, a large discrepancy appears in global mean thermosteric sea level in the 1990s. In year 1991, an observational data set, the World Ocean Data 1994 edition (WOD94), was replaced by an operational database collected by the global telecommunication system (GTS) and Japanese domestic communication lines. Regarding the latter database, an expendable bathythermograph (XBT) drop rate correction proposed by Hanawa *et al*. (1995) was not applied to the data because the data set does not store the XBT probe type. An objective analysis without this correction results in a significantly low thermosteric sea level. There is another minor discontinuity in the analysis due to replacement of SST analysis in 1995, which is used to determine mixed layer temperature in the objective analysis.

The present study uses the latest observational data set and an SST analysis: the World Ocean Data 2001 edition (WOD01; Boyer *et al*., 2001) and COBE SST (COBE: Centennial in-situ Observation Based Estimates of variability of SST and marine meteorological variables; Ishii *et al*., 2005). New monthly temperature and salinity analyses are described in Section 2, as well as changes in quality control and objective analysis schemes. Section 3 presents the analysis results, verifying them against satellite and tidal sea level observations. In addition, halosteric sea level variation, that is sea level variation due to salinity change, is also presented and compared with thermosteric sea level variation.

2. Data and Objective Analysis

The present monthly analyses described below cover the global oceans with horizontal resolution of $1° \times 1°$ for years 1945 to 2003. The analysis domain is the same as that of the previous analysis except for inclusion of the Black Sea and addition of two levels at 600 m and 700 m depths to the previous 14 levels from surface to 500 m depth.

2.1 Data

One of the major differences from the previous analysis is the use of the latest version of the observational data, climatology, and standard deviation compiled by the National Oceanographic Data Center of the National

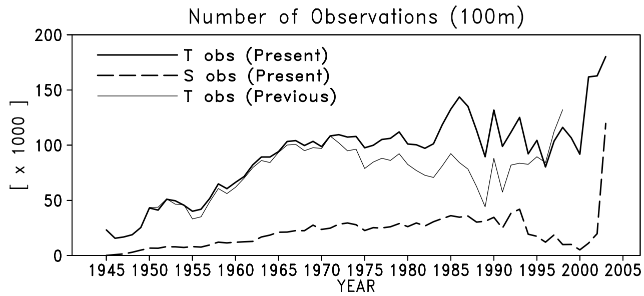

Fig. 1. Time series of the number of temperature (solid) and salinity (broken) data available at depths greater than 100 m depth. Thin solid line indicates the number of temperature data used in the previous analysis.

Ocean and Atmosphere Administrations (NODC/NOAA; Boyer *et al.*, 2001). In addition, two data sets are used; one is a database archived by the Global Temperature-Salinity Profile Program (GTSPP) of NODC which compensates for lack of data in WOD01, especially for the period of 2001–2003; the other is sea surface salinity (SSS) data compiled by IRD (L'Institut de Recherche pour le Développement, Numea, France). The GTSPP data are available from 1990 to the present, and the SSS data for 1970–2001 in the tropical and subtropical Pacific regions. The WOD01 data set includes data in the latest decades and additional data for the period of WOD94 (Fig. 1). In particular, the number of temperature observations increases from the 1970s through the beginning of the 1990s in comparison with that used in the previous analysis. In the previous analysis, the observational database for 1991–98 consists of data exchanged via GTS and domestic communication lines in Japan. Since a number of observations in seas near the Japan are available through the latter communication channels for this period, the number of temperature data used in the previous analysis is slightly larger than that in the present analysis for 1996–1998. In WOD01 for the 1950s, the date of the month is missing in more than 1000 observational reports. Such reports were unusable in the monthly analyses, because a temporal distance from the center of a calendar month is considered when defining the observational error.

In the present analysis, a new SST analysis, named COBE SST, is used throughout the period in place of the previous SST analyses of the Met Office of the United Kingdom (GISST; Global sea ice and sea surface temperature) and of the Japan Meteorological Agency. The COBE SST is based only on in-situ observation. The monthly SST analysis is produced by using reconstruction with empirical orthogonal functions computed from monthly averages of daily SST analysis by optimal interpolation, by means of variational minimization. Ishii *et al.* (2005) report that the SST analysis agrees well with another SST analysis based on satellite and in-situ observation provided by the National Centers for Environmental Prediction of NOAA (Reynolds *et al.*, 2002) in the global oceans, except for data-sparse regions south of 30°S. The COBE data set includes SST analysis errors, and these errors are utilized together with analysis errors of analyzed subsurface temperature for computation of steric sea level error.

Most of the regions in the global oceans are devoid of in-situ salinity observation, except for the last two years when the Argo buoys have been employed for temperature and salinity observations homogeneously distributed in the global oceans (The Argo Science Team, 1999; Fig. 1). To overcome this situation, several methodologies have been proposed to estimate subsurface salinity from other types of data, such as temperature, surface salinity, and sea surface height (e.g., Hansen and Thacker, 1999; Vossepoel *et al.*, 1999; Maes and Behringer, 2000). However, it is not easy for any methods to be valid for the long-term global analysis, since the salinity data necessary for the construction of the methodology are truly sparse. Therefore, no estimated salinity is used in this study.

The NODC climatology named World Ocean Atlas 2001 edition (WOA01) used in this study is defined monthly on a $1° \times 1°$ grid, and the standard deviation for seasonal average on a $5° \times 5°$ grid is adopted as in the previous study. The standard deviation mentioned formerly is denoted by σ, hereafter. Although standard deviation on a seasonal $1° \times 1°$ grid is available in WOA01, it contains a number of missing values owing to data sparseness. Hence the climatology on the high-resolution grid is not used in this study.

Analyses of temperature and salinity anomalies by NODC (Levitus *et al.*, 2005b and Boyer *et al.*, 2005; WOA05 hereafter) are used for comparison with the present analysis. Their pentadal analyses are available from 1955 to 1998, and a yearly analysis of temperature is prepared for a period of 1955–2003. These anomaly fields are computed at 28 vertical levels above 3000 m. The analyses of the upper 700 m are used for the comparison. The analysis is based on WOD01, and no estimated salinity was used as in the objective analysis of this study. In WOA05, the standard deviation check applied to all data is based on that used in WOA94 (Boyer and Levitus, 1994; Levitus, personal communication, 2005). Anomalies of observed profile at the standard levels are computed by subtracting climatology for the month in which the profile data were measured. If the anomalies exceed 3σ in open ocean regions and 5σ for observations that occur in a 5-degree square including land, the data are not used in their objective analysis. All observed anomalies available in each year or for each year-season compositing period are averaged in each 1° box at all the standard levels in the upper 3000 m. Refer to Boyer and Levitus (1994) for further details.

2.2 *Quality control*

As documented in IKK03, there are seven steps in the quality control and data selection: location check, data thinning in the vertical, comparison against SST analysis, gross error check, comparison with nearby observations, erroneous profile check, and data merging in space and time. Applying these procedures benefits homogeneity of spatio-temporal data distribution, reduction of computational cost in the objective analysis, and accuracy of resultant analyses. These procedures are also applied to salinity observation. In addition, density inversion is checked in temperature and salinity profiles. There are several changes in the above procedures, as described below.

In the new quality control, after inspecting for unrealistically large observed anomaly relative to monthly climatology, data with anomaly greater than 15σ are discarded (gross error check), while the anomaly within three standard deviation (3σ) is accepted (check A). All observations deviating by 3σ–15σ are examined by comparison with nearby observations (check B). In the gross error check, tens of data at reported levels are discarded, and most data having a large anomaly are inspected through check B. In the previous study, the thresholds were 2σ and 2–6σ respectively for checks A and B. These are rather severe criteria for data in areas with large variability, such as the tropical Pacific. In order to reduce observational noise and the computational load, multiple reports are merged into one if they are mutually close in space and time. Thresholds 1° and 1 day as criteria of closeness were adopted for the data merging in the previous study, but the temporal interval is set at 10 days in this study in order to homogenize the data distribution in time specifically for moored buoy observations and to reduce unrepresentative signals of observation more effectively. Observations near the coast were rejected in the previous analysis because the data-missing grid prevents interpolating climatology to observational location in the usual manner. However, such data are valuable in coastal areas with large variability, for example in the Kuroshio and Gulf Stream regions and off the western coast of the American Continents, and in closed seas like the Mediterranean and the Japan Seas. In this study, data near land are retained in the quality control.

About half or more of all the subsurface data is composed of XBT observations from the mid-1960s through the present. Reported data measured by specific types of XBT probe suffer from systematic errors which have been revealed in comparison with accurate CTD (Conductivity, Temperature, and Depth) observations at the same place and the same time (Hanawa *et al*., 1995). The errors originate from errors in depth estimated as a function of elapsed time after the probe is released. Such XBT data need to be corrected by using another set of drop rate parameters proposed by Hanawa *et al*. (1995). The probe types subject to this correction are *T-4*, *T-6*, *T-7*, and *DEEP BLUE*. Both of the observational data sets include flags for the correction; WOD01 provides a probe type and a flag which indicates if the correction has already been applied or not, for each XBT profile, while in the GTSPP data set there is no probe type but a code which indicates the necessity of the correction. For XBT profiles with unknown probe type, which are seen in both data sets, the correction is applied to the reports, unless the observation is made at depths greater than 840 m (Conkright *et al*., 2001). The reason for this is that an XBT probe type, *T-5*, for measurement deeper than the threshold depth is not subject to the correction. In practice, most of the XBT profiles in the observational data sets were corrected.

2.3 *Objective analysis*

Monthly departures from the WOA01 climatology are computed in the objective analysis. The analysis scheme is based on a variational minimization with spatio-temporal covariance of background error. Major differences from the previous analysis are the use of three-dimensional background error covariance, an objective analysis of salinity, and computation of isothermal layer depth (ILD) and mixed layer depth (MLD) fields prior to the temperature and salinity analysis. In this study, ILD is defined as a depth where the temperature changes by 0.5°C from SST, while MLD is a depth where the density increases by 0.125 Kg/m^3 from that at sea surface. These definitions were used by Levitus (1982) and similar definitions with various thresholds are widely used in later research. The salinity, ILD, and MLD analyses are configured in the same manner as that of the temperature analysis. The depth analyses are performed in a two-dimensional space. The SST analysis and sea surface salinity observations are incorporated in the objective analyses as observations at analysis levels shallower than analyzed ILD and MLD, respectively, whose observational errors are assumed to increase linearly with depth (see IKK03 for details). Before the use of the SST analysis in the objective analysis, differences between long-term monthly averages of the SST analysis and WOA01 are subtracted from the SST analysis. Further details of the above changes are described below. As in the previous study, analysis errors are estimated in a framework of optimal interpolation.

The background error decorrelation is a function of horizontal and vertical distances in the present analysis, while a Tikhonov term was adopted in the previous analysis scheme for vertical smoothness of the analysis outputs. The spatial decorrelation scale is assumed to vary as a function of depth, as is the temporal scale. At sea surface the scales are 300 km in the horizontal, 10 m in the vertical, and 15 days, and they increase linearly with rates of 30 km/100 m, 6 m/100 m, and 2 days/100 m, respectively. These scales are determined crudely, referring to previous studies (White, 1995; IKK03) as well as SST analysis studies (Reynolds and Smith, 1994; Ishii *et al.*, 2005). The same error covariances are used in the temperature and salinity analyses. Correlation between temperature and salinity is not considered, although temperature and salinity are analyzed simultaneously in the variational scheme.

A constraint term to determine temperature above ILD from the SST analysis (the third term on the right-hand side of equation 2 of IKK03) causes a rather severe computational burden in the variational analysis, because the data are located compactly at all ocean grid points above ILD even in the polar regions. Hence, SST data are given to the objective analysis after thinning them out. In the thinning process, local minima and maxima are picked up first in the global region, and second along the coastal grid points complementarily. The coastal SSTs are needed to produce sizable anomalies along the coasts in the analysis results. Finally, the distribution of SST data is homogenized in space so that at least one datum exists in a 3°-latitude box. Whereas the number of degrees of freedom decreases by thinning, observational errors of the SST analysis should be smaller than those of the previous analysis. The standard deviation of the error is set to 1.25σ in this study.

In the previous analysis, climatological ILD was adopted to analyze mixed layer temperature with the SST analysis. In this case, ILDs diagnosed from the temperature analysis were larger by tens of meters than observed values since the climatological temperatures are smooth in the vertical. Moreover, the ILDs suffer from spurious trends as a function of the number of data available for the objective analysis. To avoid these problems, ILD and MLD are objectively analyzed before conducting the main objective analysis. The standard deviation of depth error is roughly given by linear functions of latitude, ϕ: $10 + 20|\phi|/90$ m and $7 + 14|\phi|/90$ m, respectively for the ILD and MLD analyses. These functions are based on the standard deviation of pilot analyses with a constant depth error. The decorrelation scales of background error in space and time are the same as those for the temperature analysis. The climatologies of ILD and MLD are averages of the pilot analyses for 1961–2000. Profile data used in the depth analyses require that the maximum depth is greater than ILD and MLD, and that the profile data are reported densely enough in the vertical to determine the depths. Needless to say, such data are sparse.

Compared with the analyses adopted in WOA05, the present analysis scheme filters observational errors out more efficiently by using the objective analysis scheme, and the SST analysis is additionally used together with in-situ observations in order to compensate for data sparseness and to obtain a feasible mixed layer temperature. In addition, observed anomalies larger than 3σ are objectively inspected to see whether they are suitable for the objective analysis or not. The analysis intervals are also different between the two analyses: monthly in this study and yearly for temperature and pentadal for salinty in WOA05.

3. Results

In this section, zonal means of temperature and salinity are presented first, compared with WOA05. Next, the present temperature analysis is verified against satellite and tide gauge sea levels. Here, sea level estimated from the analysis outputs is thermosteric, that is, sea level changes only due to oceanic thermal variation, and climatological salinity is used here. The steric sea level is computed by integrating vertically specific volume relative to reference seawater. The formula of state for sea water proposed by UNESCO (Gill, 1982) are used to compute specific volume. Next, historical changes in thermosteric sea level are discussed, focusing on modifications of the quality control and objective analysis schemes as well as increase in the number of subsurface temperature observations. Finally, the role of salinity on steric sea level change, i.e., of halosteric component, is demonstrated in the latter part of this section.

3.1 Zonal mean temperature and salinity

Linear trends of zonal mean temperature and salinity are shown as a function of depth in Fig. 2 in comparison with those of the former analyses by LAB05 and Boyer *et al.* (2005), respectively. The trends shown are of the averages for all longitudes in 1955–1998. As seen from the figure, the temperature and salinity are neither increasing nor decreasing uniformly in all latitudes. Roughly speaking, areas for negative/positive temperature trend correspond to positive/negative salinity trend. This implies that the thermosteric changes are compensated by halosteric changes (Levitus *et al.*, 2005a), and such haline contraction is largely seen in high latitudes of the Northern Hemisphere (Boyer *et al.*, 2005). In general, the trends agree with each other. However, the magnitudes of the trends found in the present analysis are smaller than those of WOA05, particularly in the Southern Hemisphere. Owing to the data sparseness, the present analysis contains values close to climatology at many grids, and hence the zonal mean anomalies are close to zero. On the other hand, the zonal mean anomalies are large in WOA05 because of a simple averaging of observations available in each 1° box and each year or year-

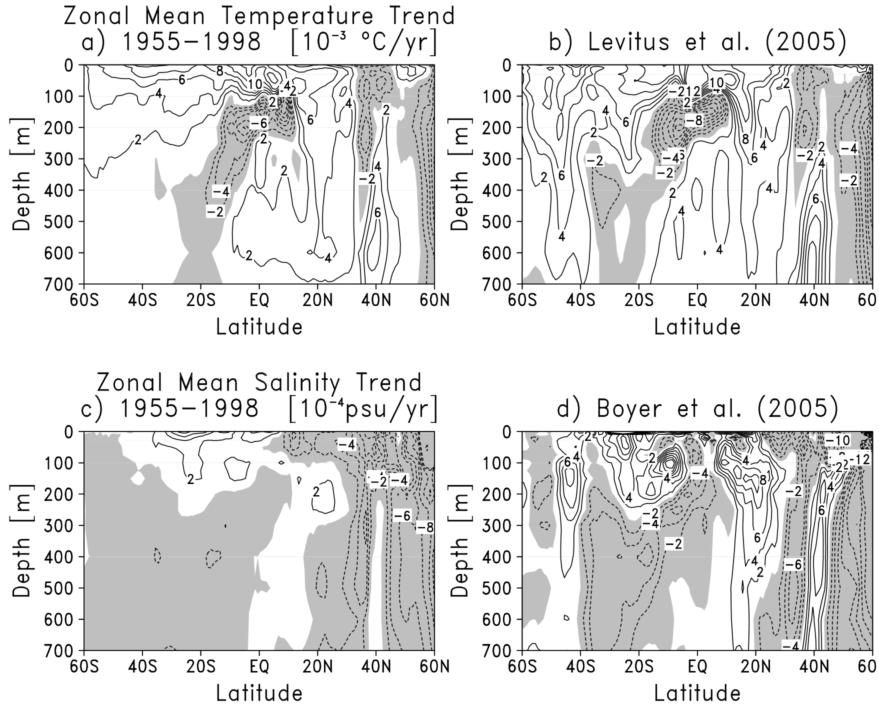

Fig. 2. Trend for zonal means of temperature (upper) and salinity (lower). The trends of the present analyses are shown in the left-hand panels in comparison with WOA05 (right). The units are 10^{-3}°C/yr and 10^{-4} psu/yr for temperature and salinity trends, respectively. Contour interval is 5 in all the panels, and negative trends are shaded.

season compositing period (Subsection 2.3). These differences in the zonal means are notable and originate from the differences in the analysis schemes. The following subsection (Subsection 3.3), discusses how the zonal mean differences affect sea level changes.

3.2 Comparison with satellite and tide gauge sea levels

The monthly temperature analysis is verified against a TOPEX/Poseidon SSH analysis by Chambers *et al*. (2003). In their SSH analysis, a trend of the TOPEX microwave radiometer equipped with the satellite is removed from the SSH observations for the period from January 1993 to February 1999, and biases caused by the reflection of the radar pulse due to surface waves, so-called sea state bias, are subtracted from observed SSHs on the basis of comparison of SSH data with tide gauge data.

Figure 3 shows geographical distributions of correlation coefficient (CC; upper) and root mean square difference (RMSD; lower) between thermosteric sea level of the present analysis (0–700 m depths) and the TOPEX/Poseidon SSH for 1993–2003. Both time series include seasonal cycles. The present analysis agrees with the SSH analysis in broad regions with CC exceeding 70% and RMSD less than 4 cm. In general, the agreement is much better in the Northern Hemisphere and the tropical oceans. In the tropics, CC reaches 90%. In Kuroshio and Gulf Stream regions, RMSDs exceed 5 cm and originate from insufficient interannual variations in the temperature analysis.

The figure is a counterpart of figure 16 of IKK03. In the previous comparison, the period was only six years from 1993 to 1998, the maximum depth of the temperature analysis was 500 m, and the SSH analysis was based on Kuragano and Shibata (1997) in which meso-scale eddies are analyzed by using 4-dimensional decorrelation scales that vary geographically. Because of the existence of meso-scale eddy, RMSDs were more than 15 cm over eddy-active regions such as regions of the Kuroshio, Kuroshio extension, and Gulf Stream. By contrast, the SSH analysis by Chambers *et al*. (2003) is used in Fig. 3. The eddies are filters out in their SSH analysis. This is a proper choice, since meso-scale eddy is not a target of the present analysis.

Shadings in the figure denote if the temperature analysis for 1993–1998 agrees with the SSH analysis or not in comparison with the previous analysis, taking the SSH analysis as reference. The thermosteric sea level is computed from temperature analysis and climatological salinity in the upper 500 m since only the temperature analysis is available at depths from sea surface to 500 m in the previous study. Correlation coefficients of the present analysis increase by more than 10% (light shad-

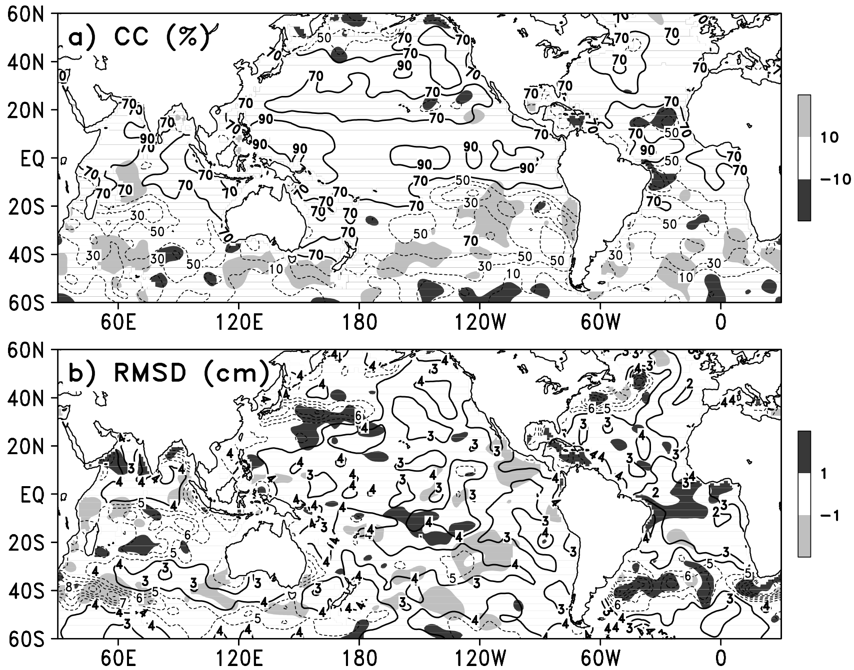

Fig. 3. Geographical distribution of a) correlation coefficient (CC; %; upper) and b) root mean square difference (RMSD; cm; lower) between the monthly thermosteric sea level and the TOPEX/Poseidon SSH analysis for 1993–2003. Both time series include seasonal cycle. The steric sea level is computed from the temperature analysis at depths from surface to 700 m depth. Contour interval in panel a is 20%. Solid contours are for CC of 70% and 90%, and broken for CC of 10%, 30%, and 50%. In panel b, counters are drawn every 1 cm by solid and broken lines respectively for RMSDs less than or equal to 4 cm and for RMSDs greater than 4 cm. Shadings denote if the present analysis agrees with the SSH analysis (light shading; increase of CC by 10%; decrease of RMSD by 1 cm) or not (dark shading; decrease of CC by 10%; increase of RMSD by 1 cm), compared with the statistics of previous analysis for the period from 1993 to 1998.

ing in panel a) in the Southern Hemisphere compared with the previous study, and root mean square differences become smaller by more than 1 cm (light shading in panel b) there as well. Comparing climatology and anomaly of the thermosteric sea level with those of SSH separately (figures not shown), half of the changes in the Southern Hemisphere are explained by changes in seasonal cycles of thermosteric sea level, and the rest by that of the interannual variations. On the other hand, the present analysis becomes worse in some areas (dark shading in panels a and b) than the previous analysis. More of observations for the 1990s are available in the present analysis in comparison with the previous analysis. In regions where meso-scale eddies are active, variances of eddy may not be filtered out in the present analysis as much as in the SSH analysis. This is because the thermosteric sea level over some regions in question are in good agreement with another SSH analysis in which meso-scale eddies are represented. Moreover, temperature variations are overestimated slightly in data sparse regions, e.g., sea level averaged over the Indian Ocean and the subtropics in the Pacific. The SST analysis used in the objective analysis has small interannual variances over the southern oceans compared with that of Reynolds *et al*. (2002), the latter of which satellite SST observation is used. Owing to this, variability of temperature within isothermal layer depth becomes small in the present analysis. This results in poor agreement in latitudes south of 50°S. Note that contribution from salinity and freshwater inputs to sea level changes is not considered in the above comparison. However, the better agreement over the southern oceans is likely to be due to the increase of observed data in WOD01 than in WOD94.

As another verification of the objective analysis, thermosteric sea level is compared with tide gauge data along the Japanese coast. Although there are more than 100 tidal stations along the coast, long-term records for about 100 years are available only at 11 stations. Even in observations of the 11 stations, data suffer from severe discontinuity, or land subsidences and upheavals due to ground water extraction and earthquakes. After removing station data unsuitable for the detection of the climate signal, five stations finally remain usable (K. Sakurai, personal communication, 2005). Three stations of the five are located on the Japan Sea side, with the remainder on the Pacific side. Before comparison with the thermosteric sea level, crustal movements are eliminated from the tide gauge data (see Appendix). The data of crustal movement are available for 1969–2000. Accordingly, the correction amount in 1969 is applied to data before 1969, and linearly extrapolated amounts are used for 2001–2003. As mentioned above, the sea level data used here are superior in quality. Hence, the resultant time series after the correction does not change significantly in comparison with the time series including crustal movement, except for one station on the Pacific side, where a trend due to crustal movement is 0.5 mm/yr.

In Fig. 4, the broken line presents 5-year running mean sea levels averaged over the above five stations. The sea level decreases from the middle of the last century, taking a local maximum in the 1970s, and it increases again from 1985 to the present. The mean thermosteric sea level, which is constructed from grid point values near the five tide gauge stations, follows the tide gauge observation well. Although the range of the crustal movement is within one standard deviation of errors estimated for the steric sea level shown by bars in the figure, the agreement becomes better than that for the case of the tidal observation without the elimination of crustal movement. Because of coarseness of the analysis grid, the thermosteric sea levels are affected by density variation far away from the coast. For this reason, interannual variations of the Kuroshio path affect the thermosteric sea levels at grid points near the tide gauge stations on the Pacific side; for instance, the Kuroshio flowed along large meander paths in the latter halves of the 1970s and the 1980s. The reason for large differences around the mid-1960s is not clear at present. The interdecadal variation of the present analysis is comparable to that of tide gauge data, while the amplitude of the previous analysis was small. This improvement is due to the use of coastal data as well as the changes in parameters of the quality control procedures in this study.

Improvement of the temperature analysis is seen at other tidal stations worldwide. Figure 5 shows root mean square difference (RMSD) and correlation coefficient

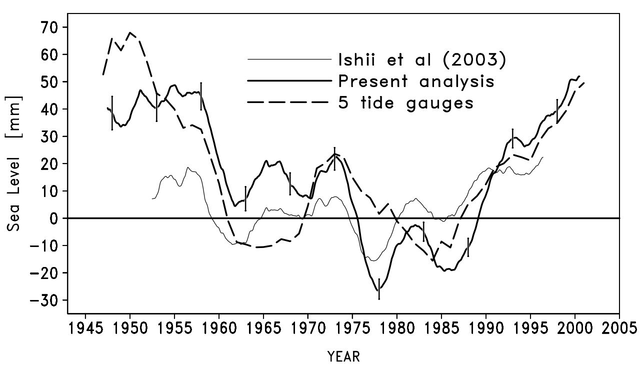

Fig. 4. Comparison with tide gauge observation along the Japanese coast. The broken line indicates long-term tidal observations at 5 station; Oshoro (34.9°N, 132.1°E), Wajima (34.9°N, 132.1°E), Hamada (34.9°N, 132.1°E), Kushimoto (33.5°N, 135.8°E), and Hosojima (32.6°N, 131.7°E). Values are 5-year running mean in mm and relative to 1961–1990 averages. Thermosteric sea levels of the previous and present analyses are shown by thin and thick solid lines, respectively. The steric sea level is computed from the temperature analysis at depths from surface to 500 m depth.

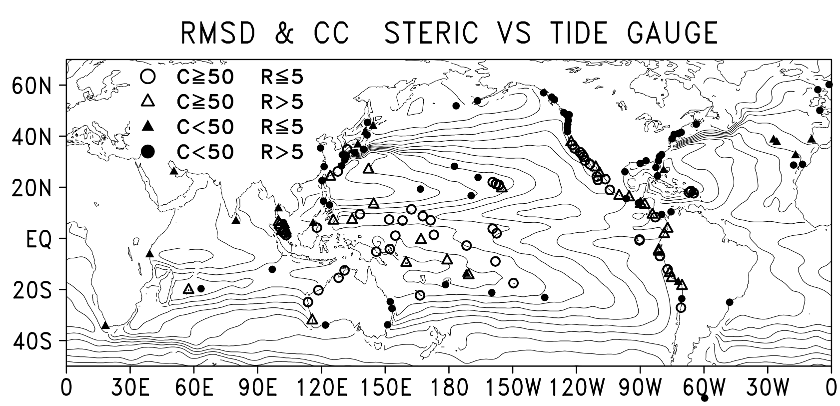

Fig. 5. Comparison of monthly thermosteric sea level anomalies with monthly tide gauge data at 168 stations where the observations are available for more than 120 months in the period from 1950 to 1998. As shown by the legend in the upper-left corner, symbols denote a combination of correlation coefficient (C) and root mean square difference (R), e.g., open circle means correlation coefficient greater than or equal to 50% and root mean square difference less than or equal to 5 cm. Thresholds 50% and 5 cm are close to the averages of the 168 tide gauges. Background contours show annual mean thermosteric sea levels every 10 cm.

(CC) between tide gauge and the thermosteric sea levels at 168 stations, where tidal data are available for more than 120 months during the period from 1950 to 1998. The tide gauge data used here are obtained from the University of Hawaii Sea Level Center. In low latitudes, CCs are mostly greater than 50%, and in particular the agreement is much better in the western and central Pacific accompanied by RMSDs of less than 5 cm. In contrast, poor agreement is caused by data sparseness and missing salinity, as discussed in IKK03. At 129 stations out of 168, CCs of the present analysis are regarded as statistically significant against those for the previous analysis at the 95% confidence level. Table 1 shows mean CCs and RMSDs for all the stations and for the stations in 20°S–20°N in comparison between the present and previous analyses. The present analysis shows good performance as the mean CCs increase by 6%, and the RMSDs reduce by 1–3 mm compared with the previous analysis. Tide gauges whose RMSDs exceed 9 cm are not included in the above comparison, since they supposedly suffer from local effects due to shallow continental shelves or crustal movement.

3.3 Thermosteric sea level changes

Figure 6 shows time series of annual mean thermosteric sea level averaged in all longitudes along three latitudinal bands; 15°N–60°N, 15°S–15°N, 60°S–15°S. The sea level is computed from the temperature analysis from surface to 500 m depth. The choice of the 500 m depth is for comparison with the previous analysis available in the upper 500 m depths.

In the figure, the present analysis (thick solid line) is compared with the previous analysis (thin solid) and a temperature analysis by LAB05 (dotted) for the period between 1955 and 2003, and with a sea surface height (SSH) analysis of TOPEX/Poseidon by Chambers *et al.* (2003) for 1993–2003 (broken). Error bars in the figure denote one standard deviation, which are computed from the monthly analysis errors available at each grid point.

The thermosteric sea levels vary dominantly on decadal and interdecadal time scales with periods of 5–20 yrs, and increasing trends are commonly seen in the three latitudinal bands. As for the northern oceans (panel a), the amplitude of the decadal change grows since 1945, and the global mean sea level is rising from the middle of

Table 1. Statistics between thermosteric sea level anomalies and tide gauge data at stations located in latitudes from 60°S to 60°N (left-hand columns) and from 20°S to 20°N (right-hand columns). The number of stations is 168 for the former latitudinal range and 78 for the latter. The table contains correlation coefficients (CC in %) and root mean square differences (RMSD in mm) averaged data at all the stations in each latitudinal range.

	60°S–60°N		20°S–20°N	
	CC	RMSD	CC	RMSD
Present analysis	46	57	58	51
Previous analysis	40	58	52	54

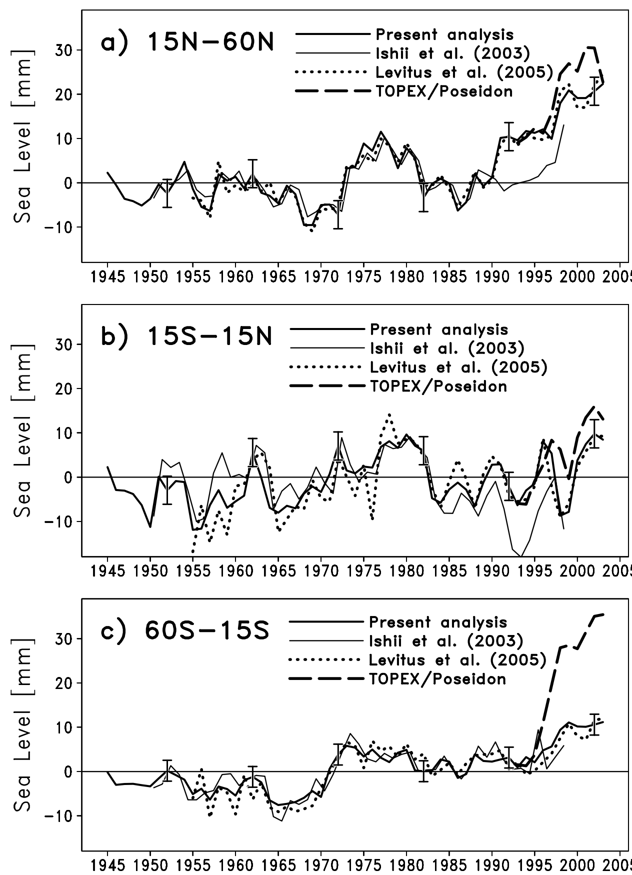

Fig. 6. Time series of annual mean thermosteric sea level (mm) averaged along three latitudinal bands; 15°N–60°N, 15°S–15°N, and 60°S–15°S, for years from 1945 to 2003. Thin and thick solid lines indicate the previous and present analysis, respectively. Time series of Levitus *et al.* (2005b) and the TOPEX/Poseidon SSH analysis by Chambers *et al.* (2003) are shown respectively by dotted and broken lines. The analysis by Levitus *et al.* is available from 1955 to 2003, and the SSH data are shown from 1993 to 2003. The thermosteric sea levels are computed from the temperature analysis from sea surface to 500 m depth. All values shown are relative to 1961–1990 averages of each time series. In case of the TOPEX/Poseidon SSHs, the value in January 1993 is adjusted to the mean of thermosteric sea levels of the present analysis and Levitus *et al.*'s. Error bars drawn every 10 years are of the present analysis and denote error intervals of one standard deviation.

the 1980s to the end of 2003. Owing to El Niño and Southern Oscillation, larger interannual changes appear in sea level in the lower latitudes (panel b) than in other latitudinal domains. In the southern oceans (panel c), an increasing trend of sea level rise for the entire period is statistically significant, but is the smallest among the three time series. The present analysis agrees well with the LAB05 analysis despite many differences between the analyses schemes adopted by LAB05 and this study. Throughout the period, some discrepancies appear between the present and the LAB05 analyses, although the same observational database is used. However, in most years, the differences are within the 95% confidence interval, that is, about twice as large as those indicated by the error bar. Year-to-year changes in the thermosteric sea levels are slightly smaller than LAB05's. Heat content is also computed from the temperature analyses by integrating the product of specific heat, density, and temperature vertically. The resultant heat contents show similar curves to those in Fig. 6.

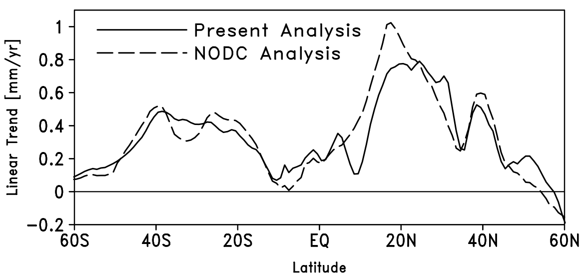

Fig. 7. Trends of zonally averaged thermosteric sea level (mm/yr) for the present analysis (solid line) and Levitus *et al*. (2005a) (dashed), corresponding to the trends of temperature and salinity shown in the Fig. 2.

Although the linear trends of zonal mean temperature are very different in the southern oceans (Fig. 2), small differences are seen between steric sea level of Levitus *et al*. (2005a) shown by a dashed line and the present analysis (solid). One reason for this is that density is insensitive to temperature change in latitudes south of 50°S where temperature is low. Large variability is seen in year-to-year change in the thermosteric sea level of Levitus *et al*. (2005b) over the southern oceans owing to the variety of vertical temperature anomalies. As a result, the trend of steric sea level is not large, as expected from the temperature trend (Fig. 2b). In contrast, the zonal mean steric sea level of the present analysis increases rather monotonically (figures not shown). These facts reflect the differences in methodology of the two historical analyses (Section 2). For the reasons mentioned above,

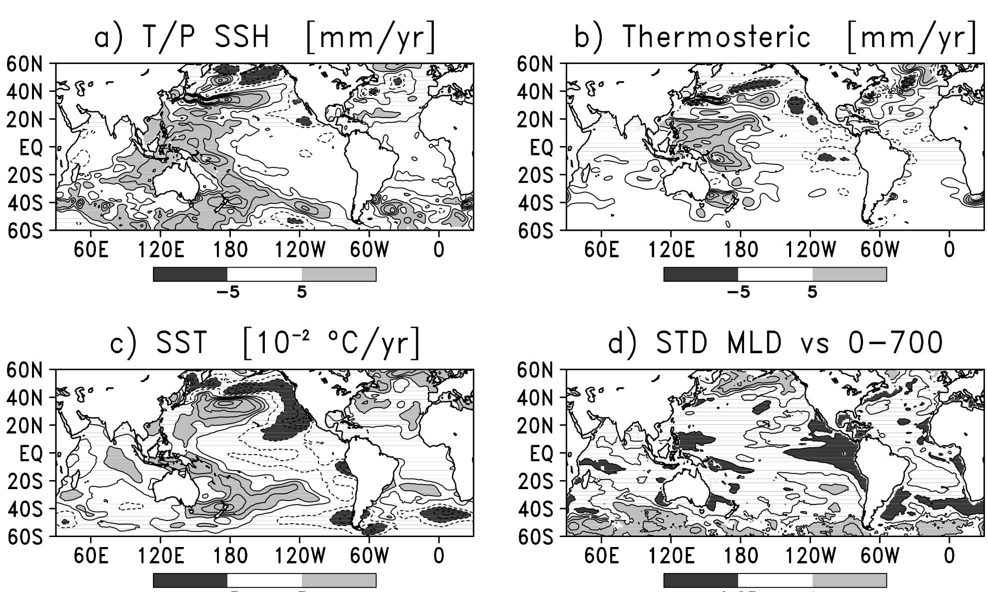

Fig. 8. Geographical distribution of linear trend of a) the satellite sea level (mm/yr), b) thermosteric sea level (mm/yr), and c) SST (10^{-2}°C/yr). Contour intervals are 2.5 mm/yr for sea level and 0.025°C/yr for SST. Light and dark shadings are applied for trends of sea level less than –5 mm/yr and greater than 5 mm/yr, respectively, in panels a and b, and for SST trends less than –0.05°C/yr and greater than 0.05°C/yr, respectively, in panel c. Contours for trend of zero are not shown, and negative trends are represented by broken lines. Panel d shows ratio of STDs for thermosteric sea level computed from temperature within isothermal layer depth to those for all the levels. Contours are drawn for 0.25, 0.5, 1, 2, and 4. The period of the statistics is from 1993 to 2003.

a local peak of trend of zonally averaged thermosteric sea level appear around 40°S (Fig. 7; Antonov *et al.*, 2005). In Fig. 7, differences between the trend of the present analysis (solid line) and WOA05 (dashed) correspond to trends in zonal mean temperatures shown in Fig. 2.

In the case of the present analysis, a linear trend of global mean thermosteric sea level is estimated to be 0.36 mm/yr ± 0.07 mm/yr for the period between 1955 and 2003, and that for heat content is $0.19 \times 10^{22} \pm 0.05$ J/yr. These trends are nearly the same as the estimates by LAB05 and Antonov *et al.* (2005). Here, the trends of thermosteric sea level and heat content are computed from the temperature analysis at all levels from sea surface to 700 m depth, unlike those in Fig. 6. For the recent 11 years, the thermosteric sea level trend of the present analysis is 1.2 ± 0.3 mm/yr. The trend is also comparable to that of LAB05, while the trend of the satellite sea level is computed as 2.9 ± 0.6 mm/yr.

According to our computation, global mean thermosteric sea level declines by about 10 mm, when the XBT drop rate correction is withheld from all XBT data. As described in Section 1, there are severe gaps in the previous analysis (thin line in Fig. 6) in comparison with LAB05 in latitudes north of 15°S during the 1990s.

The TOPEX/Poseidon SSH increases more rapidly since the mid-1990s than the thermosteric sea level of the present analysis. The satellite sea level shows significant sea level rise (SLR) in both the northern and southern oceans (panels a and c of Fig. 6). These SLR values may not be represented in the temperature analyses with sparse observations, particularly in the southern oceans. Eustatic effects on SLR, such as fresh water input (Antonov *et al.*, 2002) and glacier melting, are not considered here, either. Furthermore, salinity variations may also affect them to some extent, as will be discussed later. In the tropical and subtropical Atlantic Ocean, SLR is much smaller in comparison with the satellite SSH after the mid 1990s. This is a primary reason for lower steric sea level anomalies for 15°S–15°N than the SSH anomalies (panel b).

The sea level trend is not uniform over the global oceans (Fig. 8), while the trends of zonal mean temperature and salinity are (Fig. 2). Compared with linear trends of the satellite sea level (panel a), the thermosteric sea level trends are underestimated mostly in the global oceans from 60°S to 60°N, although Willis *et al.* (2004) pointed out that missing salinity information may yield an overestimate of sea level trend in middle and high latitudes. Levitus (1989) and Antonov *et al.* (2002) reported that density compensating changes occur over relatively large ocean areas and Levitus *et al.* (2005a) stated that large regions of the world ocean demonstrate either density compensating changes in temperature and salinity or changes acting in concert to change sea level. Moreover, non-steric effects should be considered (Antonov *et al.*, 2002) here. As shown in Fig. 6, the agreement of linear trend is good in the Northern Hemisphere, while it is poor in the southern oceans. The use of SST analysis to determine temperature within the isothermal layer depth (ILD) possibly compensates for data sparseness to some extent in high latitudes since ILDs reach hundreds of meters in wintertime. Actually, linear trends of the SST analysis (panel c) resemble those of sea level in their global spatial patterns, while some differences between the two analyses are seen, for instance, along the western boundary currents and in middle and high latitudes. In order to see how the sea level variation is affected by temperature changes above ILD, standard deviations (STDs) of thermosteric sea level computed from temperatures in ILD are compared with those computed from temperature above the 700 m depth. Panel d of Fig. 8 shows the ratio of the former to the latter. A ratio of 100% denotes that the temperature changes above ILD explains one half of the total sea level change. A ratio of more than 100% appears in high latitudes, and it is less than 50% mostly in middle and low latitudes. Note that STDs multiplied by the square root of layer thickness are compared in the figure, and that temperatures for isothermal layers are analyzed not only with the SST analysis but also with in-situ observations. From panels c and d, it is hard for SST analysis to fully explain the trend of sea level, even in high latitudes. Moreover, unlike the SSH trends shown in panel a, positive trends of SST are not dominant in the Indian and Pacific sections of the southern oceans, and negative SST trends appear in the Atlantic Ocean south of 40°S. Regarding sea level changes in the southern oceans, temperature variations below ILD may be too small to explain the satellite sea level changes. Moreover, temperature changes below 700 m depth and salinity variations or any other non-steric effects can also be the contributing factors.

3.4 *Effects of salinity*

Owing to the sparseness of salinity observations, halosteric sea levels are poorly reproduced in this analysis. Furthermore, discussion of the short-term trend of the salinity analysis will be misleading; for instance, linear trends in the halosteric component over local regions for the last 10 years are unacceptable since spatio-temporal distribution of salinity observation changes drastically owing to the increase of Argo salinity (cf., Fig. 1).

In order to see the thermosteric and halosteric effect on sea level changes, steric sea level h for a given temperature and salinity profile (**T** and **S**, respectively) is decomposed into climatological, thermosteric, and halosteric components as

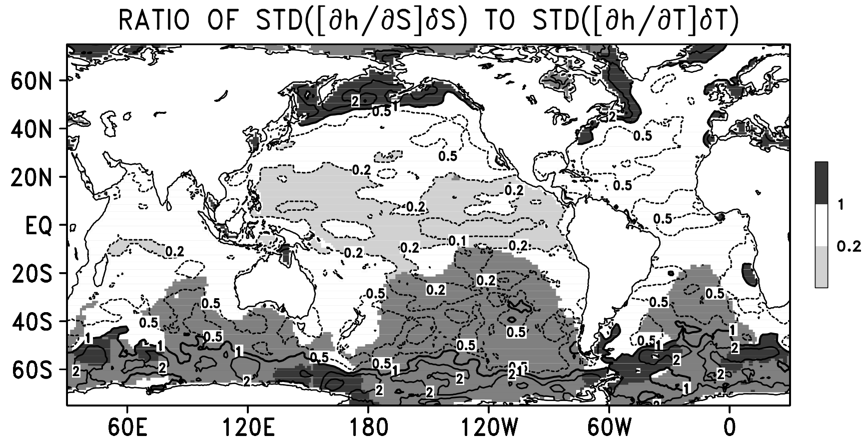

Fig. 9. Ratio of halosteric component to thermosteric component. Contours drawn are of ratio 0.1, 0.2, 0.5, 1, 2, 5, and light and dark shades indicate ratio less than 0.2 and greater than 1, respectively. Sparse sampling areas are shown by shading with moderate darkness.

$$h(\mathbf{T},\mathbf{S}) = h(\mathbf{T}^c,\mathbf{S}^c) + \sum_k \left.\frac{\partial v_k}{\partial T_k}\right|_{\substack{T_k=T_k^c\\ S_k=S_k^c}} \left(T_k - T_k^c\right)\delta z_k + \sum_k \left.\frac{\partial v_k}{\partial S_k}\right|_{\substack{T_k=T_k^c\\ S_k=S_k^c}} \left(S_k - S_k^c\right)\delta z_k$$

by linearization about a climatological temperature and salinity profile ($\mathbf{T^c}$ and $\mathbf{S^c}$, respectively), where suffix k indicates the vertical level number, v_k is specific volume computed from local temperature and salinity, and the δz_k denotes layer thickness. This approach is similar to that of Antonov *et al*. (2002). After computing the thermosteric and halosteric components from the monthly temperature and salinity analyses, standard deviations (STDs) of the thermosteric and halosteric components for 1961–2000 are compared. Here, temperature and salinity climatologies are the averages of the analyses for 1961–2000. Figure 9 shows the ratio of halosteric STD to thermosteric STD nearly over the global oceans. The computation of STDs was done using the analyses only at grid points with neighboring observations available in the monthly analysis, that is, where the analysis errors of temperature and salinity are reduced at least by 2.5% at all the depths from the standard deviation of background error.

A meridional contrast and some characteristic features are apparently seen in the figure; the thermosteric component is dominant in low latitudes, especially in the tropical and subtropical regions of the Pacific and Indian Oceans, while the halosteric STDs exceeds thermosteric STDs in high latitudes, particularly along sea-ice margins and closed seas (dark shades). In addition, the role of salinity on steric changes appears to be more important in the Atlantic Ocean than in other oceans since the ratio is about 0.5 broadly, even in the tropical and subtropical Atlantic Ocean, and less than or about 0.2 over other oceans in low latitudes. These patterns reflect vertical patterns of temperature and salinity variations and of climatological states in each region. The figure suggests an intrinsic role of salinity on sea level change. In Fig. 3, root mean square differences normalized by the standard deviation of interannual SSH anomaly are large in high latitudes and over the Atlantic Ocean rather than in other oceans (additional figures not shown). Therefore, the halosteric component should not be ignored when discussing steric sea levels distributed geographically, as done in Figs. 3 and 8. A similar image to that in the figure can be obtained by computing directly from observed temperature and salinity profiles. However, the result will be much more noisy than that shown in the figure.

In order to see how much the halosteric component affects global mean steric sea level, the time series of the halosteric component is compared with that of the thermosteric component (Fig. 10). The values plotted are averages in all longitudes from 60°S to 60°N. Unlike the statistics shown in Fig. 9, the steric sea levels at all the grid points are used in averaging. The global mean steric sea level appears to be determined primarily by the thermosteric component. This result is the same as that reported by Antonov *et al*. (2002). The linear trend of thermosteric and halosteric components for 1954–2003 is 0.31 ± 0.07 mm/yr and 0.04 ± 0.01 mm/yr, respectively. These estimates are close to those of WOA05 produced by Levitus *et al*. (2005b) and Boyer *et al*. (2005), respectively. Note that the salinity analysis is close to climatol-

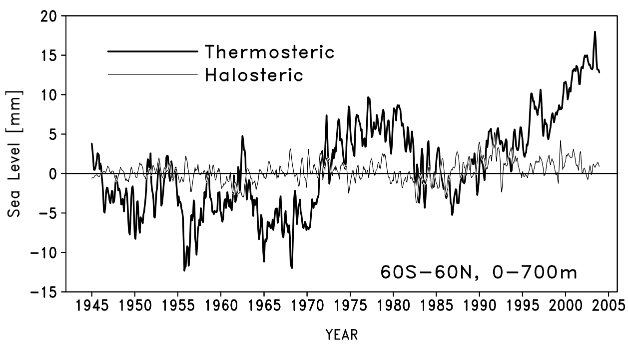

Fig. 10. Time series of the monthly halosteric (thick) and thermosteric (thin) components averaged in all longitudes from 60°S to 60°N.

ogy widely in the global oceans for all the period, except after 2001. In the above estimate, the halosteric trend is 10 times smaller than thermosteric trend. Meanwhile, negative trends of salinity should be caused by sources of freshwater other than melting sea ice, and additions of freshwater to the oceans result in sea level rise. As Antonov *et al.* (2002) pointed out, sea level rise due to additions of freshwater to the global oceans, which are equivalent to observed salinity changes, are substantial.

4. Concluding Remarks

The objective analysis of monthly temperature and salinity has been carried out with the aim of reproducing the spatial distribution of the variables and their local changes on interannual and interdecadal time scales. Steric sea level changes are mainly discussed using the monthly subsurface temperature and salinity analysis which is a revised version of Ishii *et al.* (2003). The analyses are carried out using the variational minimization scheme with the World Ocean Data 2001 edition, IRD sea surface salinity data, and the SST analysis of Ishii *et al.* (2005). The present analysis covers the topmost 700 m of the global ocean from 1945 to 2003. The analysis and quality control schemes are mostly the same as those of the previous analysis, except for minor changes in quality control and data selection procedures. The drop rate correction has been applied to XBT data that are subject to the correction. Without the correction, a significant gap of about ten millimeters appears in the global mean thermosteric sea level as in the previous analysis. The new monthly analysis presents reasonable global mean variations of steric sea level for recent 59 years. Use of observations near coasts yields realistic fluctuations of the analyzed temperatures.

The trends of steric sea level estimated from the present analysis are comparable to WOA05 by Boyer *et al.* (2005) and Antonov *et al.* (2005). The analyzed fields of temperature and salinity are generally smooth rather than those of WOA05, since the quality control and analysis schemes adopted in this study are constructed so as to filter out observational noise more than in WOA05. In addition, the linear trends of zonally averaged temperature and salinity are smaller than theirs. A large discrepancy is found in the time series during the recent 11 years between the thermosteric sea level and the satellite sea surface height (SSH), especially in the southern oceans. The thermosteric trends may be underestimated in the southern oceans owing to data sparseness (Lombard *et al.*, 2005). Salinity variability is one of the contributing factors in steric sea level, in particular, in high latitudes and the Atlantic Ocean according to the estimation of this study (Fig. 9). The SST variations in high latitudes affect sea level changes largely since the mixed layer depth is great; they explain more than 50% of the standard deviation of thermosteric sea level variation at latitudes greater than 50° (Fig. 8). However, the geographical patterns of SST trend are not necessarily the same as those of sea level. Part of the differences of thermosteric sea level from SSH (Fig. 6) may be caused by insufficient representation around the Antarctic Circumpolar Current (ACC). Gille (2002) reported warming at a rate of 0.004°C/yr on average in 700–1100 m along ACC from the 1950s to the 1980s. This layer is not the target of the present objective analysis. When temperature increases by 0.1°C from climatology uniformly in this layer, thermosteric sea level would rise by about 5 mm.

In turn, non-steric effects should be considered when comparing steric sea level with tide gauge data and SSH observations. Recent publications (Antonov *et al.*, 2002; Levitus *et al.*, 2005a) have proposed a guideline to interpret underestimation of thermosteric sea level against sea level rise detected by tide gauge and the SSH data. If the temperature and salinity analyses were true, non-steric components would be significantly large in the southern oceans (Fig. 6). However, there is no answer to this at present, including spatial distributions of non-steric components. Further investigation is needed for quantitative understanding of sea level variations over each ocean basin.

In this study, local changes in the thermosteric sea level are compared with the tide gauge data along the Japanese coast, eliminating crustal movement from 1969 to 2003. The comparison shows that the thermosteric component is dominant in the sea level change around Japan. As for tide gauges in the global oceans, the agreement is better in areas where the thermosteric components are regarded as a dominant factor in steric sea level change as shown in Fig. 9. In the mean time, tide gauge data are useful for discussions of secular change in sea level and are actually utilized in a number of climate studies. However, any discussion of them should take care to account

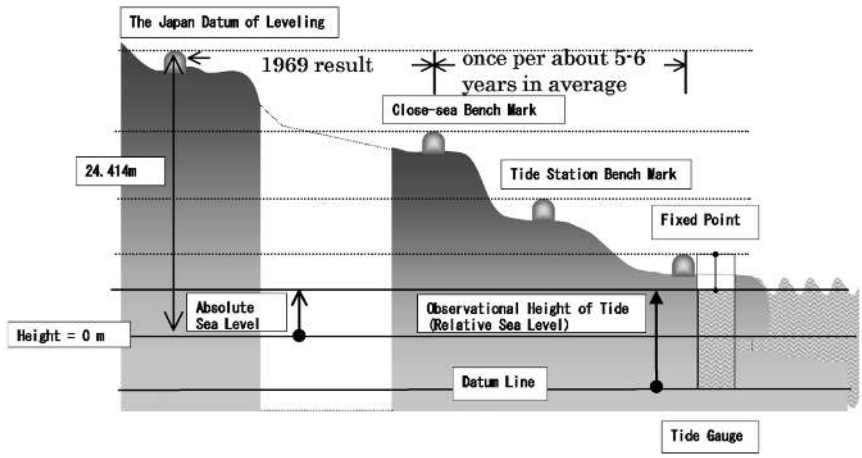

Fig. A1. Relationship between leveling bench marks and tide gauge observation. See text for details.

for crustal movement, at least in the Japanese tide gauges. At several stations used in Fig. 4, differences between thermosteric sea level and tide gauge data are large before 1969, possibly because the data of crustal movement are not available.

The new data set contains analysis errors as well as analyzed values, as did the previous data set. It is hoped that the analysis is applicable to studies to detect long-term variability in the global oceans, such as global warming and sea level rise. There still remains room for improvement in the objective analysis. In order to produce month-to-month persistent anomalies and more spatio-temporal variability, it may be effective to use analysis at the previous time step as the first guess, as Reynolds and Smith (1994) did.

Acknowledgements

The authors wish to thank the distributors of WOD01 and climatologies and anomaly fields of WOA05 (Dr. Levitus, NODC/NOAA/USA; http://www.nodc.noaa.gov/), the TOPEX/Poseidon SSH analysis (CSR, the University of Texas, USA; http://www.csr.utexas.edu/sst/), and tide gauge data (the University of Hawaii Sea Level Center; http://www.soest.hawaii.edu/kilonsky/uhslc.html). They appreciate the excellent investigation of the previous analysis by Drs. A. Cazenave and A. Lombard (CNES/France), who provided many hints for improvement of the analysis. Their appreciation is extended to Mr. K. Sakurai (Office of Marine Prediction, JMA) for valuable information on the sea level changes along the Japanese coast. Prof. Hanawa (Tohoku Univ.) encouraged the authors in completing the manuscript. The thoughtful and constructive comments of two anonymous reviewers are thankfully acknowledged. This work was partially supported by the Japan Science and Technology Agency through the Core Research for Evolutional Science and Technology.

Appendix. Elimination of Crustal Movement

In Japan, tide level is presented as a value measured from the datum line (DL) fixed at each tide gauge. DL is connected to the Japan Datum of Leveling, that is, the origin of ground leveling of Japan, via close sea bench marks and fixed points of tide gauges (Fig. A1) As tide gauges are constructed on the ground, the presented tide values contain effects of crustal movements and oceanic origin sea level changes. Japan is located in a geologically highly active region. To reduce the crustal movement effects, ground leveling has been done every 5 or 6 years on average from fixed points to close sea bench marks. Ordinarily, the distances from fixed points to close sea bench marks are 2–6 km. But, the distance from the Japan Datum of Leveling to close sea bench marks is sometimes over 1000 km. So the heights of close sea bench marks are not revised very frequently because the compilation of ground leveling data needs much time. Actually, the latest revision was made by the Geological Survey of Japan in 2000 and the second latest one was made in 1969. But the ground leveling has been done continuously and the results are compiled as Height Difference Data. We made calculations to get time series of height of close sea bench marks using Height Difference Data directly. To minimize errors, we took a loop route for the calculations and fixed error criteria as $2.5S^{1/2}$ mm, where S is the distance measured along the loop route in km. If the height difference of a bench mark at the beginning and after the calculation along the loop route is over the criteria, we adopt another loop route until the error meets the criteria. The total amount of error is distributed to the bench marks' height of the loop route proportionally to the distance of the bench marks along the loop route. These calculations were made all around Japan and the time series of the height of close sea bench marks were determined.

References

Antonov, J. I., S. Levitus and T. P. Boyer (2002): Steric sea level variations during 1957–1994: Importance of salinity. *J. Geophys. Res.*, **107**(C12), 8013, doi:10.1029/2001JC000964.

Antonov, J. I., S. Levitus and T. P. Boyer (2005): Thermosteric sea level rise, 1955–2003. *Geophys. Res. Lett.*, **32**, L12602, doi:10.1029/2005GL023112.

Boyer, T. P. and S. Levitus (1994): *Quality Control and Processing of Historical Oceanographic Temperature, Salinity, and Oxygen Data*. NOAA Technical Report NESDIS 81, 64 pp.

Boyer, T. P., M. E. Conkright, J. I. Antonov, O. K. Baranova, H. Garcia, R. Gelfeld, D. Johnson, R. Locarnini, P. Murphy, T. O. Brien, I. Smolyar and C. Stephens (2001): *World Ocean Database 2001, Volume 2: Temporal Distribution of Bathythermograph Profiles*. NOAA Atlas NESDIS 43, 119 pp., CD-ROM, U.S. Government Printing Office, Washington, D.C.

Boyer, T. P., S. Levitus, J. I. Antonov, R. A. Locarnini and H. E. Garcia (2005): Linear trends in salinity for the World Ocean, 1955–1998. *Geophys. Res. Lett.*, **32**, L01604, doi:10.1029/2004GL021791.

Cazenave, A. and R. S. Nerem (2004): Present-day sea level change: observations and cause. *Rev. Geophys.*, **42**, RG3001, doi:10.1029/2003RG000139.

Chambers, D. P., S. A. Hayes, J. C. Ries and T. J. Urban (2003): New TOPEX sea state bias models and their effect on global mean sea level. *J. Geophys. Res.*, **108**(C10), 3305, doi:10.1029/2003JC001839.

Church, J., J. M. Gregory, P. Huybrechts, M. Kuhn, K. Lambeck, M. T. Nhuan, D. Qin and P. L. Woodworth (2001): Changes in sea level. In *Climate Change 2001: The Scientific Basis, Contribution of Working Group I to the Third Assessment Report of the Intergovernmental Panel on Climate Change*, ed. by J. T. Houghton *et al.*, Cambridge Univ. Press, New York.

Conkright, M. E., R. A. Locarnini, H. E. Garcia, T. D. O. Brien, T. P. Boyer, C. Stephens and J. I. Antonov (2001): *World Ocean Atlas 2001: Objective Analyses, Data Statistics, and Figures*. NOAA Atlas NESDIS 42, 17 pp., CD-ROM, U.S. Government Printing Office, Washington, D.C.

Derber, J. C. and A. Rosati (1989): A global oceanic data assimilation technique. *J. Phys. Oceanogr.*, **19**, 1333–1347.

Douglas, B. C. and W. R. Peltier (2002): The puzzle of global sea level rise. *Phys. Today*, **55**, 35–40.

Ghil, M. and P. Malanotte-Rizzoli (1991): *Data Assimilation in Meteorology and Oceanography*. Advances in GEOPHYSICS, Vol. 33, Academic Press, p. 141–266.

Gill, A. E. (1982): *Atmosphere-Ocean Dynamics*. International Geophysics Series, Academic Press.

Gille, S. (2002): Warming of the southern ocean since the 1950s. *Science*, **295**, 1275–1277.

Hanawa, K., P. Raul, R. Bailey, A. Sy and M. Szabados (1995): A new depth-time equation for Sippican or TSK T-7, T-6, and T-4 expendable bathythermographs (XBTs). *Deep-Ses Res.*, **42**, 1423–1451.

Hansen, D. V. and W. C. Thacker (1999): Estimation of salinity profiles in the upper ocean. *J. Geophys. Res.*, **104**(C4), 7921–7933.

Ishii, M., M. Kimoto and M. Kachi (2003): Historical ocean subsurface temperature analysis with error estimates. *Mon. Wea. Rev.*, **131**, 51–73.

Ishii, M., A. Shouji, S. Sugimoto and T. Matsumoto (2005): Objective analyses of SST and marine meteorological variables for the 20th century using ICOADS and the Kobe Collection. Int. *J. Climatol.*, **25**, 865–879.

Kuragano, T. and A. Shibata (1997): Sea surface dynamic height of the Pacific Ocean derived from TOPEX/POSEIDON altimeter data: Calculation method and accuracy. *J. Oceanogr.*, **53**, 585–599.

Levitus, S. (1982): *Climatological Atlas of The World Ocean*. NOAA Prof. Paper No. 13, 173 pp., U.S. Government Printing Office, Washington, D.C.

Levitus, S. (1989): Interpentadal variability of temperature and salinity at intermediate depths of the north Atlantic Ocean, 1970–74 versus 1955–1959. *J. Geophys. Res.*, **94**(C5), 6091–6131.

Levitus, S., C. Stephens, J. I. Antonov and T. P. Boyer (2000): *Yearly and Year—Season Upper Ocean Temperature Anomaly Fields, 1948–1998*. NOAA Atlas NESDIS 40 (available from http://www.nodc.noaa.gov/OC5/PDF/ATLAS/nesdis40.pdf).

Levitus, S., J. I. Antonov, T. P. Boyer, H. E. Garcia and R. A. Locarnini (2005a): Linear trends of zonally averaged thermosteric, halosteric, and total seteric sea level for individual ocean basins and the world ocean, (1955–1959)–(1994–1998). *Geophys. Res. Lett.*, **32**, L16601, doi:10.1029/2005GL023761.

Levitus, S., J. I. Antonov and T. P. Boyer (2005b): Warming of the world ocean, 1955–2003. *Geophys. Res. Lett.*, **32**, L02604, doi:10.1029/2004GL021592.

Lombard, A., A. Cazenave, P.-Y. Le Traon and M. Ishii (2005): Comtribution of thermal expansion to present-day sea-level change revisited. *Global and Planetary Change*, **47**, 1–16.

Maes, C. and D. Behringer (2000): Using satellite-derived sea level and temperature profiles for determining the salinity variability: A new approach. *J. Geophys. Res.*, **105**(C4), 8537–8457.

Peltier, W. R. (2001): Global isostatic adjustment and modern instrumental records of relative sea level history, Chapter 4. In *Sea Level Rise: History and Consequences*, ed. by B. C. Douglas, M. S. Kearney and S. P. Leatherman, Academic Press, New York.

Reynolds, R. W. and T. M. Smith (1994): Improved global sea surface temperature analyses using optimum interpolation. *J. Climate*, **7**, 929–948.

Reynolds, R. W., N. A. Rayner, T. M. Smith, D. C. Stokes and W. Wang (2002): An improved in-situ and satellite SST analysis for climate. *J. Climate*, **15**, 1609–1625.

Stephens, C., S. Levitus, J. I. Antonov and T. P. Boyer (2001): The Pacific regime shift. *Geophys. Res. Lett.*, **28**, 3721–3724.

The Argo Science Team (1999): ARGO: The global array profiling floats. In *Proceedings of the OOPC/UDP Ocean Obs Conference*, Saint Raphaël, France, 18–22 October, 1999, 12 pp.

Vossepoel, F. C., R. W. Reynolds and L. Miller (1999): Use of sea level observations to estimate salinity variability in the tropical Pacific. *J. Atmos. Ocean. Tech.*, **16**, 1401–1415.

White, W. B. (1995): Design of a global observing system for gyre-scale upper ocean temperature variability. *Prog. Oceanogr.*, **36**, 169–217.

Willis, J. K., D. Roemmich and B. Cornuelle (2004): Interannual variability in upper ocean heat content, temperature, and thermosteric expansion on global scales. *J. Geophys. Res.*, **109**, C12036, doi:10.1029/2003JC002260.